eLIFE
elifesciences.org

Figures and figure supplements

MicroRNAs down-regulate homologous recombination in the G1 phase of cycling cells to maintain genomic stability

Young Eun Choi, et al.

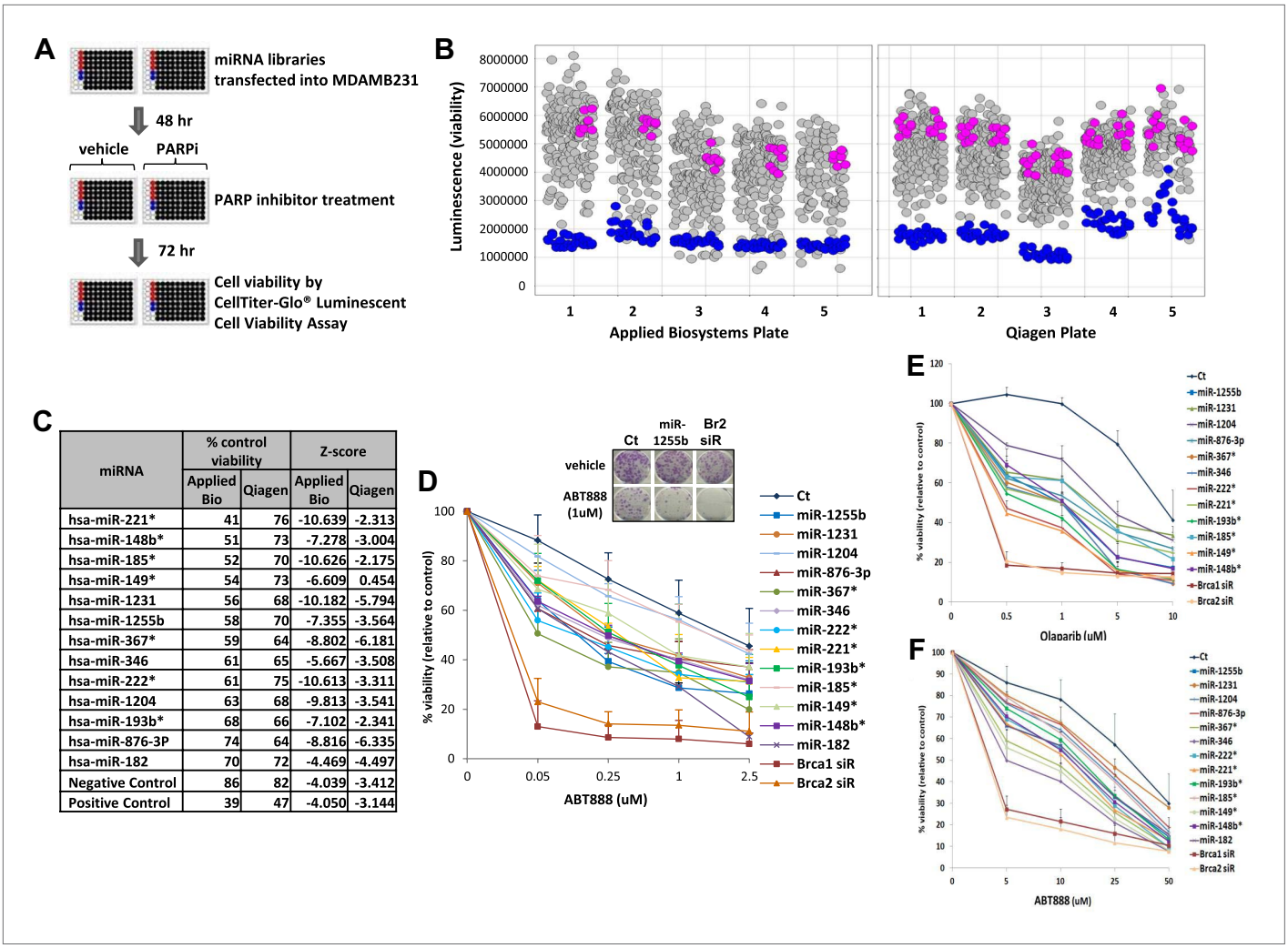

C

miRNA	% control viability		Z-score	
	Applied Bio	Qiagen	Applied Bio	Qiagen
hsa-miR-221*	41	76	-10.639	-2.313
hsa-miR-148b*	51	73	-7.278	-3.004
hsa-miR-185*	52	70	-10.626	-2.175
hsa-miR-149*	54	73	-6.609	0.454
hsa-miR-1231	56	68	-10.182	-5.794
hsa-miR-1255b	58	70	-7.355	-3.564
hsa-miR-367*	59	64	-8.802	-6.181
hsa-miR-346	61	65	-5.667	-3.508
hsa-miR-222*	61	75	-10.613	-3.311
hsa-miR-1204	63	68	-9.813	-3.541
hsa-miR-193b*	68	66	-7.102	-2.341
hsa-miR-876-3P	74	64	-8.816	-6.335
hsa-miR-182	70	72	-4.469	-4.497
Negative Control	86	82	-4.039	-3.412
Positive Control	39	47	-4.050	-3.144

Figure 1. miRNA screen for PARP inhibitor sensitivity. (**A**) Schematic of a gain-of-function screen using miRNA mimic libraries from Applied Biosystems and Qiagen to identify miRNAs that sensitize cells to the PARP inhibitor, ABT888. (**B**) Scatter plot (wells/plate) of luminescence (y-axis) as a read-out for viability of each miRNA-transfected well (grey circle) in the presence of ABT888 (20 μM). The plates are numbered in the x-axis. Positive control (BRCA2 siRNA, blue circles) and negative controls (control mimics, pink circles) are shown. Scatter plot for untreated samples is shown in ***Figure 1—figure supplement 1***. (**C**) List of top miRNAs from the screen displayed in the order of % control viability along with Z-score. (**D**) Clonogenic survival assay to validate the impact of selected miRNAs on sensitivity to ABT888. MDAMB231 cells were transfected with control miRNA mimics, indicated miRNA mimics, BRCA1 siRNA, or BRCA2 siRNA and treated with vehicle or ABT888, before measuring colony formation. Curves were generated from three independent experiments and a representative image of colony formation with 1 μM ABT888 is shown in the inset. (**E** and **F**) Luminascence-based viability assay was performed in MDAMB231 cells with PARP inhibitor, olaparib (**E**) or in 21NT cells with ABT888 (**F**). Cells were transfected with control miRNA, indicated miRNA mimics, BRCA1 siRNA, or BRCA2 siRNA and treated with vehicle or PARP inhibitor before ATP quantification. Curves were generated from three independent experiments.

DOI: 10.7554/eLife.02445.003

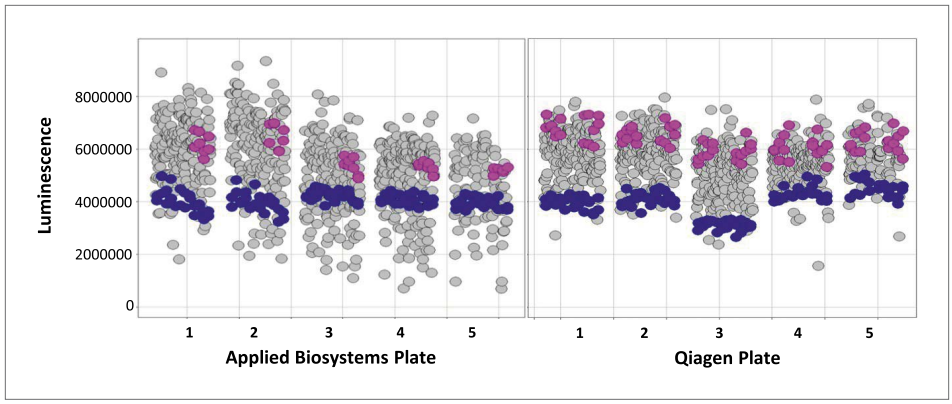

Figure 1—figure supplement 1. miRNAs screen for PARP inhibitor sensitivity.

DOI: 10.7554/eLife.02445.004

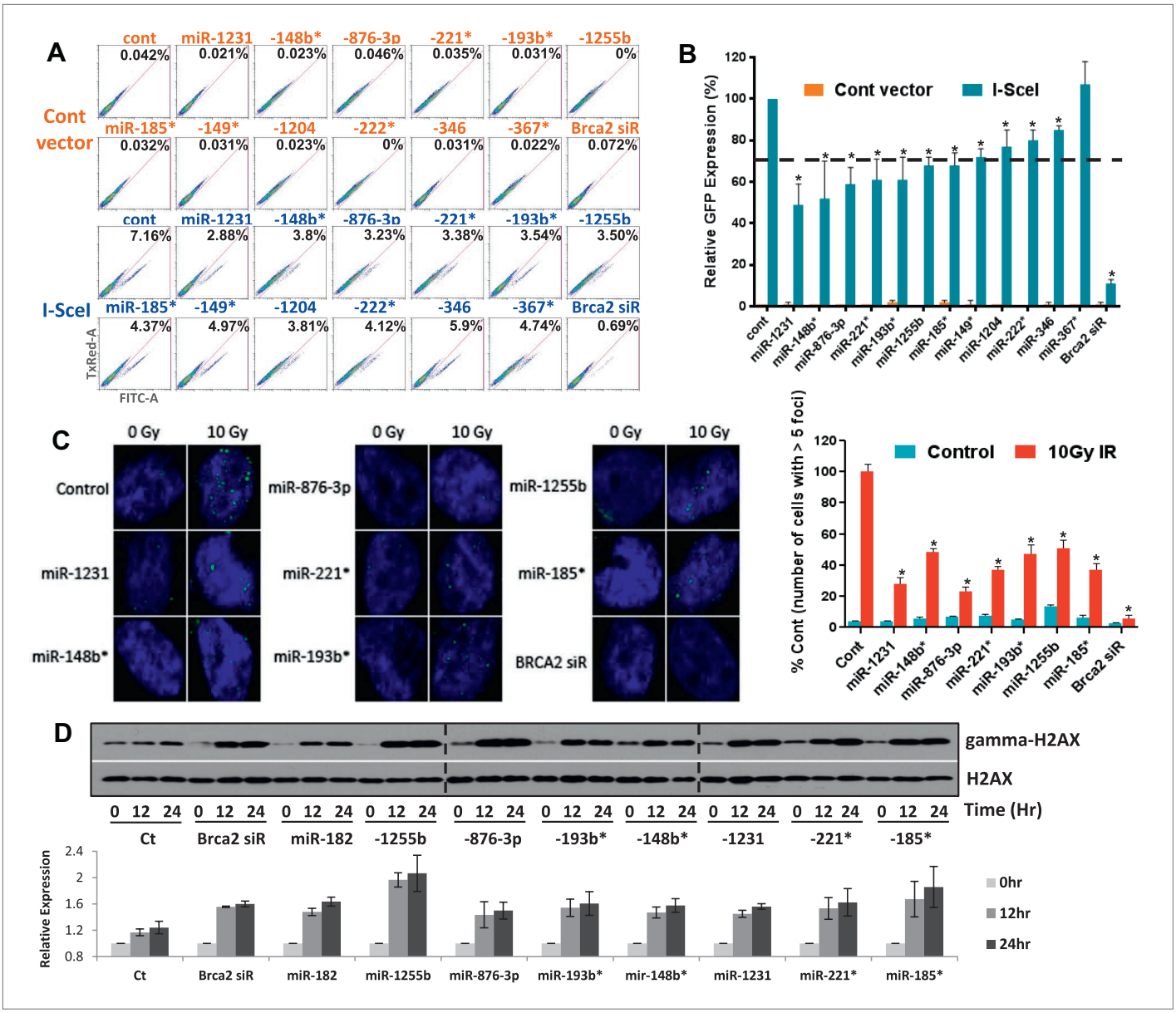

Figure 2. miRNAs sensitize cells to PARP inhibitors by targeting HR-mediated DSB repair. (**A** and **B**) Measurement of HR-mediated repair of an I-SceI induced site-specific DSB. Cells carrying a single copy of the recombination substrate (DR-GFP) were transfected with control miRNA mimic, indicated miRNA mimics, or BRCA2 siRNA before transfection with I-SceI or control vector. GFP positive cells were analyzed 48 hr later by flow cytometry (FACS). Representative images of the FACS profile are shown in (**A**), and the mean ± SD of six independent experiments is graphically represented in (**B**). The dotted line represents the cut-off which was set at 70% of the control. (**C**) Analysis of HR-mediated repair by RAD51 focus formation. MDA-MB231 cells were transfected with control miRNA mimic, indicated miRNA mimics, or BRCA2 siRNA, stained for RAD51 (green) and 4′,6-diamidino-2-phenylindole (DAPI) (blue) 6 hr after exposure to IR. The images were captured by fluorescence microscopy and RAD51 focus-positive cells (with >5 foci) were quantified by comparing 100 cells. Mean ± SD of three independent experiments is shown in right panel. * indicates $p<0.05$. (**D**) γ-H2AX accumulation after treatment with ABT888. Cells were transfected with control miRNA mimic, indicated miRNA mimics, or BRCA2 siRNA and treated with ABT888 (100 μM) before evaluation of γ-H2AX by immunoblotting at indicated time points. Total H2AX served as loading control for these experiments. Images were quantified by ImageJ software and the mean ± SD of three independent experiments is graphically shown.

DOI: 10.7554/eLife.02445.005

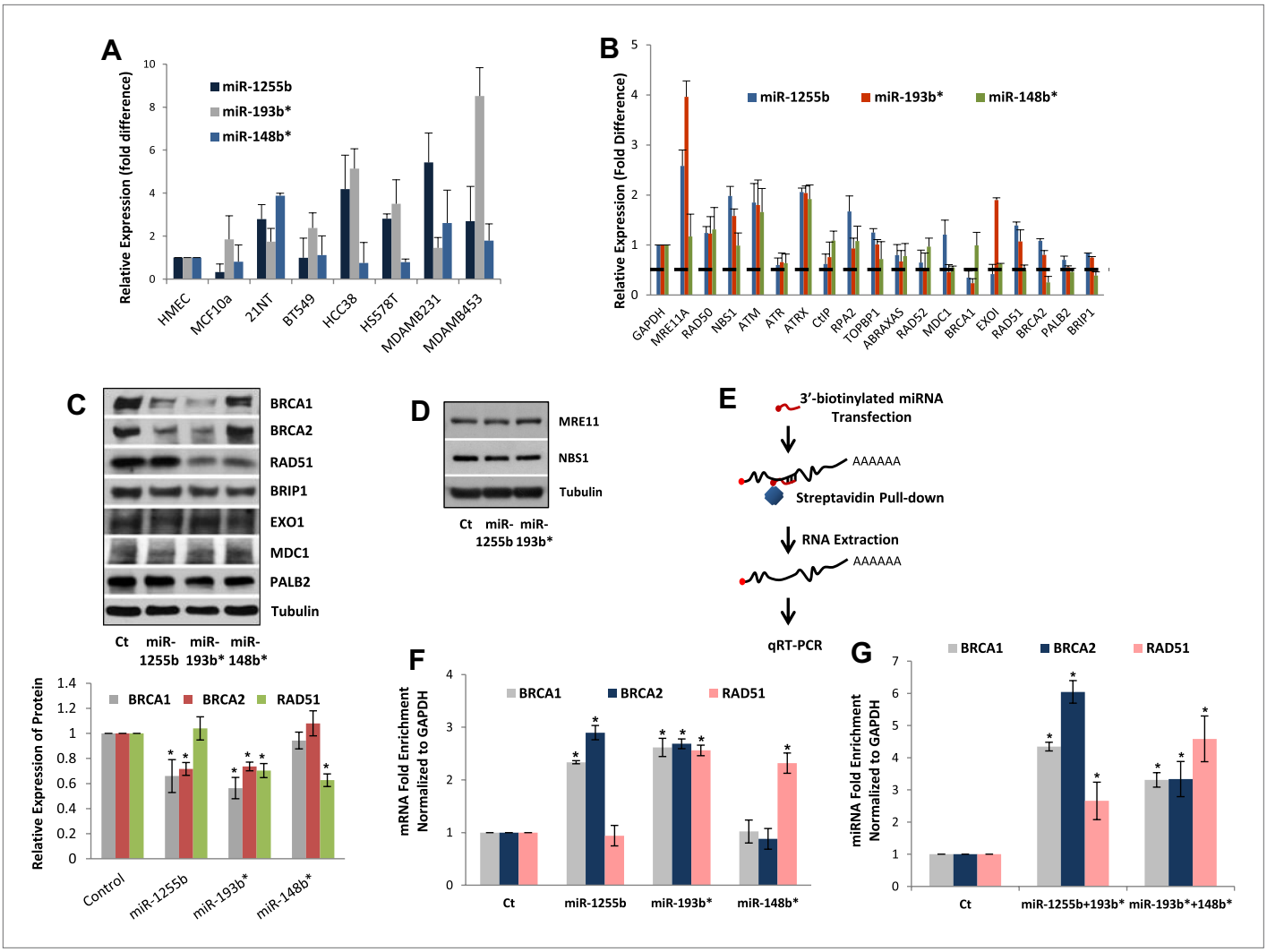

Figure 3. miR-1255b, miR-193b*, and miR-148b* regulate PARP inhibitor sensitivity by regulating expression of HR factors in TNBCs. (**A**) miRNA expression profile in a panel of breast cancer lines. Endogenous expression of indicated miRNAs was quantified by qRT-PCR (normalized to 5srRNA) and represented relative to non-tumorigenic breast epithelial cell, HMEC. Expression of miR-1255b, miR-193b*, and miR-148b* were detected in these lines. Mean ± SD of four independent experiments is shown. (**B**–**D**) Expression of DDR genes is impacted by miR-1255b, miR-193b*, and miR-148b*. MDA-MB231 cells were transfected with control mimic or mimics for miR-1255b, miR-193b*, and miR-148b* and mRNA levels of predicted and prioritized DDR genes were analyzed by qRT-PCR using gene-specific primers and normalized to GAPDH. Mean ± SD of three independent experiments is shown (**B**). (**C** and **D**) Cell lysates were then analyzed by immunoblot for factors which had ≥50% reduction in mRNA in cells transfected with miR-1255b, miR-193b*, and miR-148b*. Images were quantified by ImageJ software and the mean ± SD of three independent experiments is graphically shown, * indicates $p<0.05$. (**E**–**G**) Interaction of target transcripts with miR-1255b, miR-193b*, and miR-148b*. MDA-MB231 cells were transfected with biotinylated-control mimics or biotinylated mimics for miR-1255b, miR-193b*, and miR-148b* as a single (**F**) or a combination (**G**). The immunoprecipitated RNA was analyzed by qRT-PCR using gene-specific primers and normalized to GAPDH. Mean ± SD of three independent experiments is shown and statistical significance of enrichment of specific gene transcripts is indicated by * ($p<0.05$). The principle steps of the method are illustrated in ***Figure 3E***.

DOI: 10.7554/eLife.02445.006

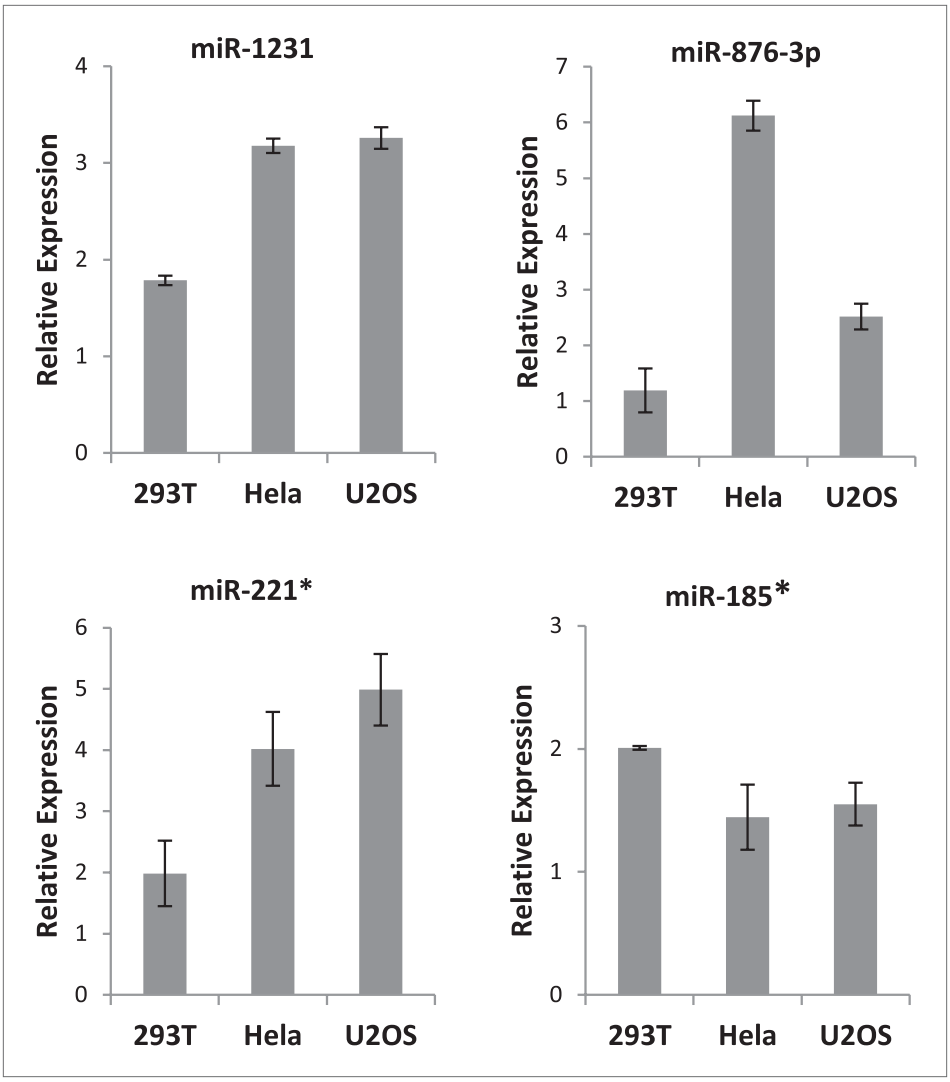

Figure 3—figure supplement 1. Expression of the excluded miRNAs.

DOI: 10.7554/eLife.02445.007

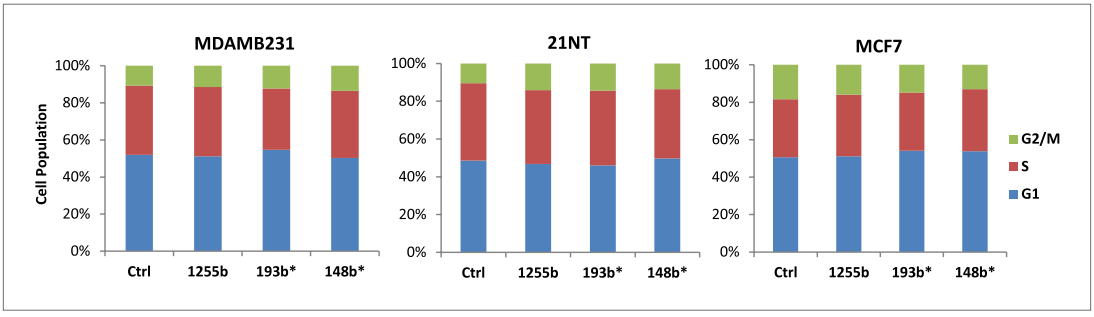

Figure 3—figure supplement 2. The effect of miRNAs on cell cycle.

DOI: 10.7554/eLife.02445.008

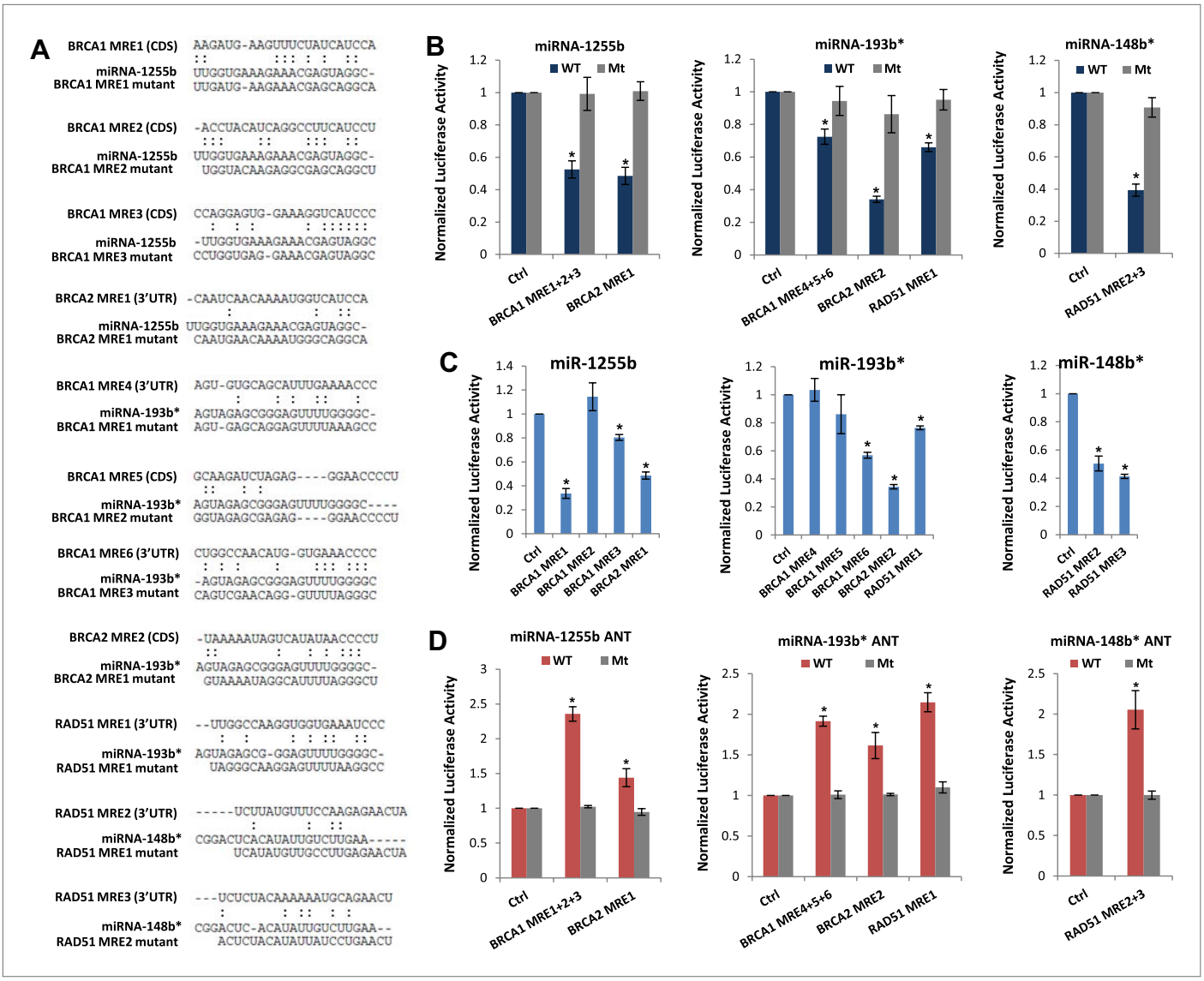

Figure 4. Predicted miRNA recognition sites (MREs) of miRNAs and their impact on targets. (**A**) Predicted MREs were obtained from PITA (http://genie.weizmann.ac.il/pubs/mir07/mir07_prediction.html) and their mutants were generated by mutating nucleotides providing complementarity and G-U wobble to corresponding miRNAs. The region where MRE is located in the gene is indicated in the parentheses. CDS: coding sequence, 3'UTR: 3' untraslated region. (**B**) Luciferase reporter assay to assess direct interaction of miR-1255b, miR-193b*, and miR-148b* with BRCA1, BRCA2, and RAD51. Combinations of predicted miRNA recognition sites (MREs) for each putative target transcript of miR-1255b, miR-193b*, and miR-148b* were cloned into the luciferase reporter vector and transfected in MDA-MB231 cells along with the indicated miRNA mimics. *Renilla* luciferase activity of the reporter was measured 48 hr after transfection by normalization to an internal *firefly* luciferase control. Mean ± SD of three independent experiments is shown and statistical significance is indicated by * ($p<0.05$). (**C**) Luciferase reporter assay for individual MREs for each target of miRNAs was performed in the same way as described in ***Figure 4B***. Mean ± SD of three independent experiments is shown and statistical significance is indicated by *($p<0.05$). (**D**) Luciferase reporter assay with miR-1255b, miR-193b*, and miR-148b* ANTs. Combinations of predicted miRNA recognition sites (MREs) in the luciferase vector for each putative target transcript of miR-1255b, miR-193b*, and miR-148b* were transfected in MDA-MB231 cells along with the indicated miRNA ANTs. *Renilla* luciferase activity of the reporter was measured 48 hr after transfection by normalization to an internal *firefly* luciferase control. Mean ± SD of three independent experiments is shown and statistical significance is indicated by *($p<0.05$).

DOI: 10.7554/eLife.02445.009

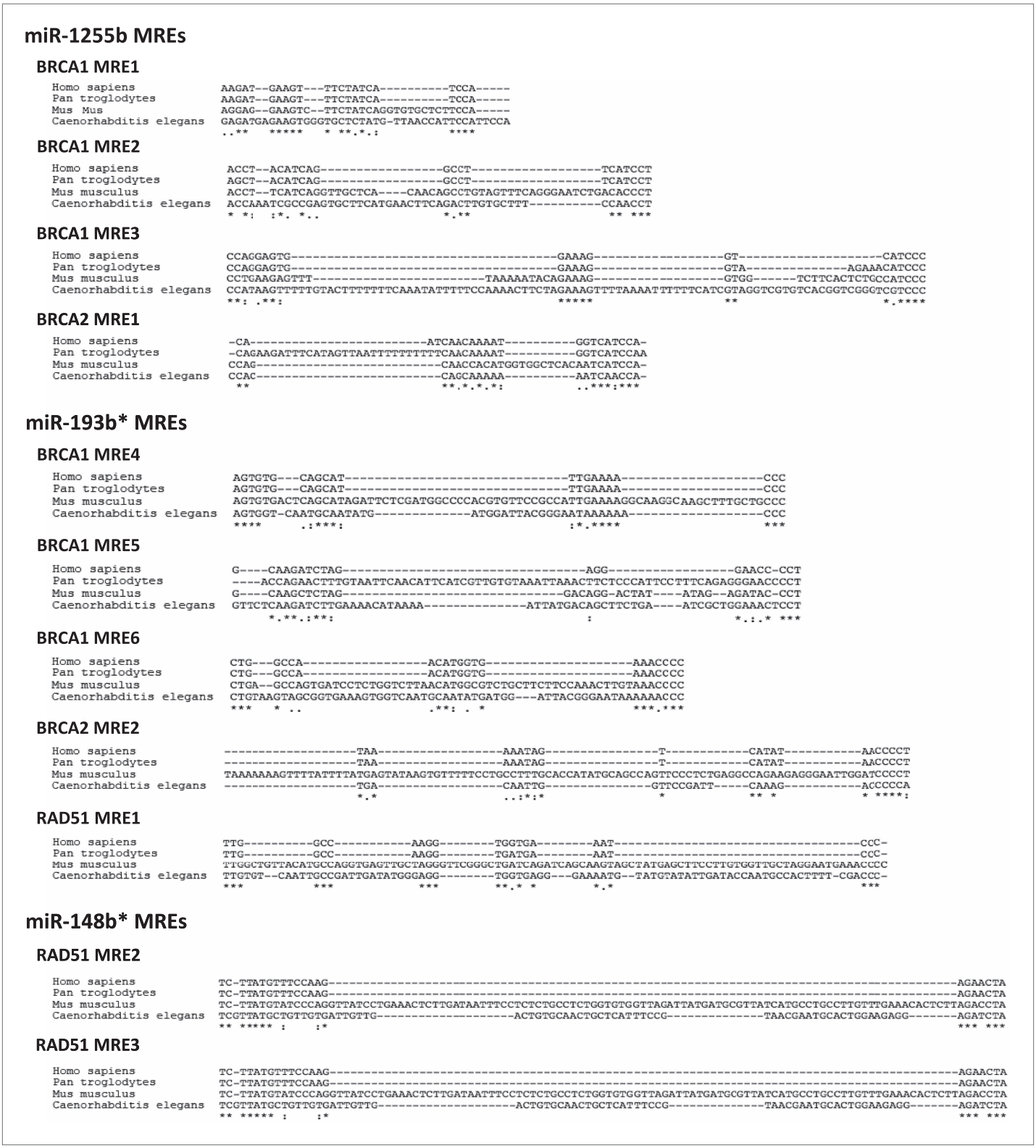

Figure 4—figure supplement 1. Conservation of predicted miRNA recognition sites (MREs) of miRNAs.

DOI: 10.7554/eLife.02445.010

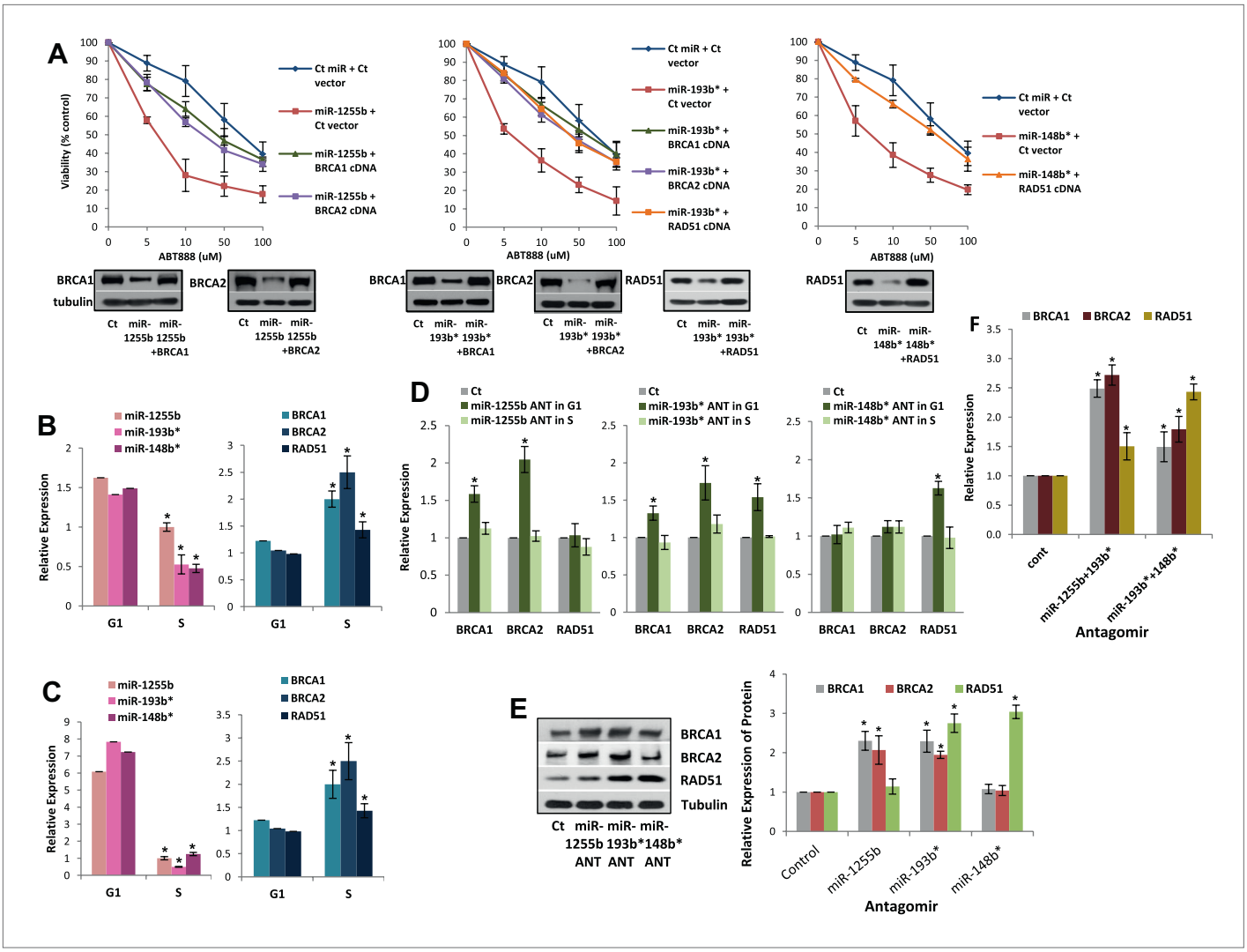

Figure 5. Impact of miRNAs on DSB repair in different phases of the cell cycle. (**A**) Rescue of the impact of miRNAs on ABT888 sensitivity. MDAMB231 cells were transfected with control miRNA or indicated miRNA mimics with or without target gene cDNAs (lacking MREs) and treated with vehicle or ABT888, before viability assay by ATP quantification. Expression of each target protein is examined by immune blot. (**B** and **C**) Expression of miRNAs and target transcripts in synchronized cells. MDAMB231 (**B**) or MCF10A (**C**) cells were synchronized with mimosine and the relative amount of miR-1255b, miR-193b*, and miR-148b* or BRCA1, BRCA2, and RAD51 mRNA for G1- or S-phase was determined by qRT-PCR (normalized to RNU1 or GAPDH, respectively). Mean ± SD of three independent experiments is shown and statistical significance is indicated by *($p<0.05$). (**D**–**F**) Impact of inhibiting miRNAs on targets in G1 cells. MDAMB231 cells were transfected with control ANT or ANTs for miR-1255b, miR-193b*, and miR-148b* as a single (**D**) or a combination (**F**). Subsequently, the cells were synchronized with mimosine and BRCA1, BRCA2, and RAD51 mRNA was assessed by qRT-PCR (normalized to GAPDH) in the G1 and/or S-phase (**D** and **F**). Cell lysates from G1 cells were analyzed by immunblot for BRCA1, BRCA2, and RAD51 (**E**). Images were quantified by ImageJ software and the mean ± SD of three independent experiments is shown, * indicates $p<0.05$.

DOI: 10.7554/eLife.02445.011

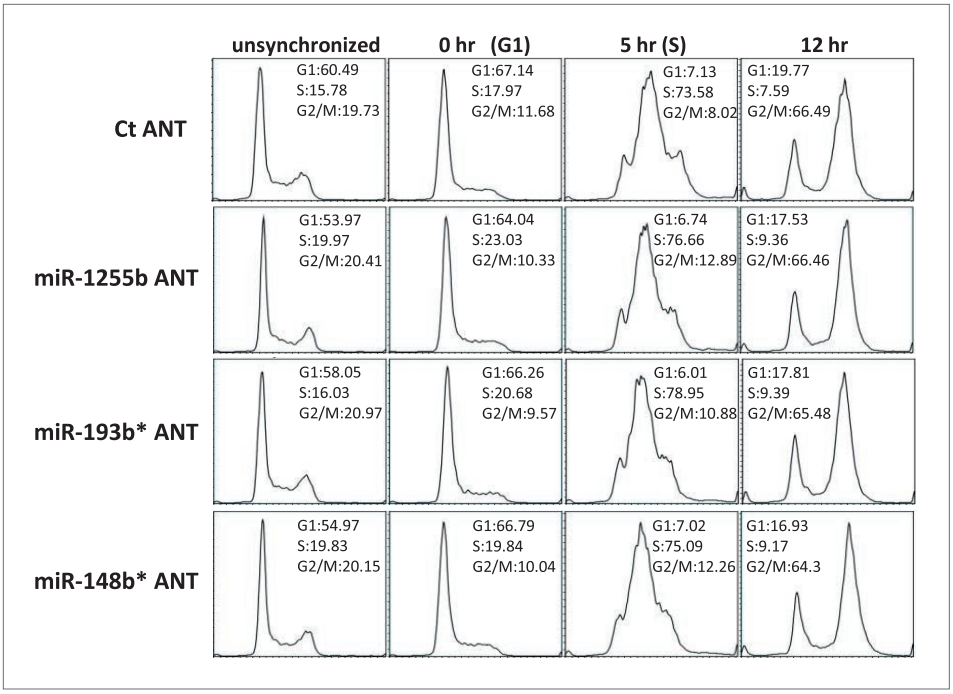

Figure 5—figure supplement 1. The impact of miRNA antagomirs (ANTs) on cell cycle progression.
DOI: 10.7554/eLife.02445.012

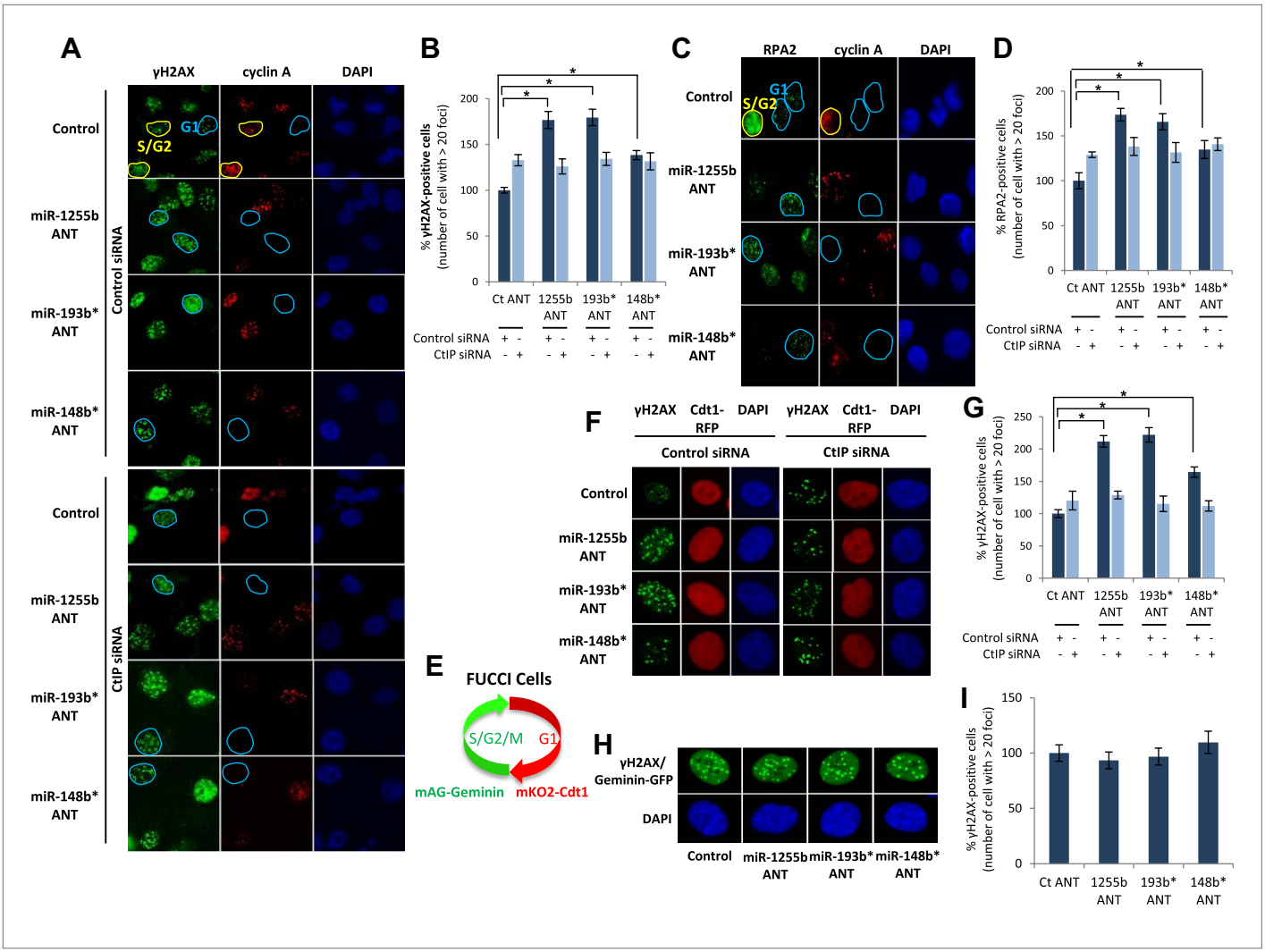

Figure 6. Impact of inhibiting miRNAs on DSB repair. (**A**–**D**) Impact of inhibiting miRNAs on DSB repair in the G1 phase of MDA-MB231 cells. Cells were transfected with control ANT or ANTs for miR-1255b, miR-193b*, and miR-148b* with or without 20 nM CtIP siRNA, exposed to IR (5 Gy) and stained for γ-H2AX (green) (**A**) or RPA2 (green) (**C**), cyclin A (red) and 4′,6-diamidino-2-phenylindole (DAPI) (blue). The images were captured by fluorescence microscopy and the number of γ-H2AX foci (**A**) or RPA2 foci (**C**) was calculated from 100 cells. Mean ± SD of three independent experiments is graphically represented (**B** and **D**). * indicates $p<0.05$. (**E**–**I**) Impact of inhibiting miRNAs on DSB repair in different phase of RPE-1 cells. RPE-1 cells expressing the Fucci system (illustrated in ***Figure 6E***) were transfected with control ANT or ANTs for miR-1255b, miR-193b*, and miR-148b* with or without 20 nM CtIP siRNA, exposed to IR (5 Gy) and stained for γ-H2AX (green) and 4′,6-diamidino-2-phenylindole (DAPI) (blue). The images were captured by fluorescence microscopy and the number of γ-H2AX foci in G1 cells (red, mKO2-Cdt1) was calculated from 100 cells (**F** and **G**). The images were captured by fluorescence microscopy and the number of γ-H2AX foci (green foci) in S/G2/M cells (green background, mAG-Geminin) was calculated from 100 cells (**H**). Mean ± SD of three independent experiments is graphically represented (**I**). * indicates $p<0.05$.

DOI: 10.7554/eLife.02445.013

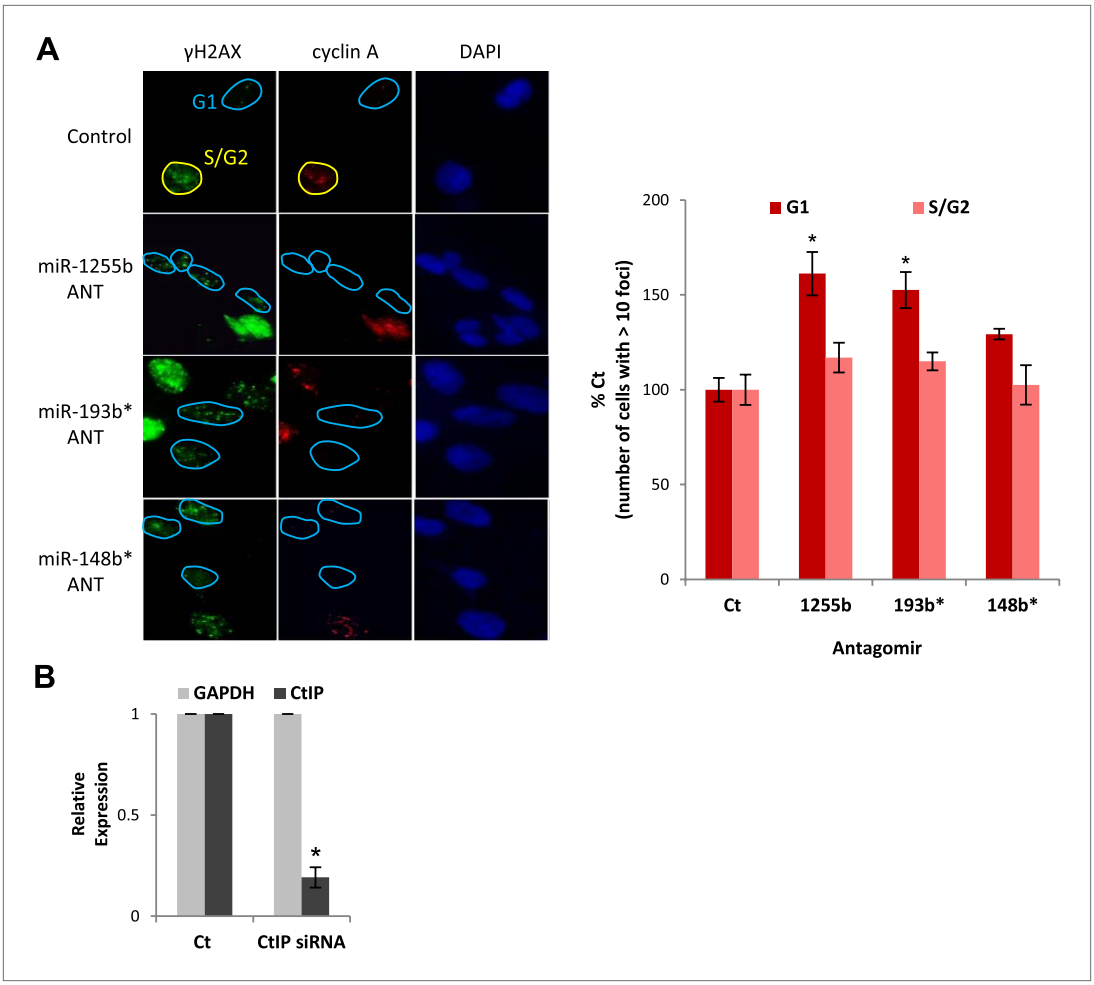

Figure 6—figure supplement 1. The impact of miRNAs on DNA repair during cell cycle.

DOI: 10.7554/eLife.02445.014

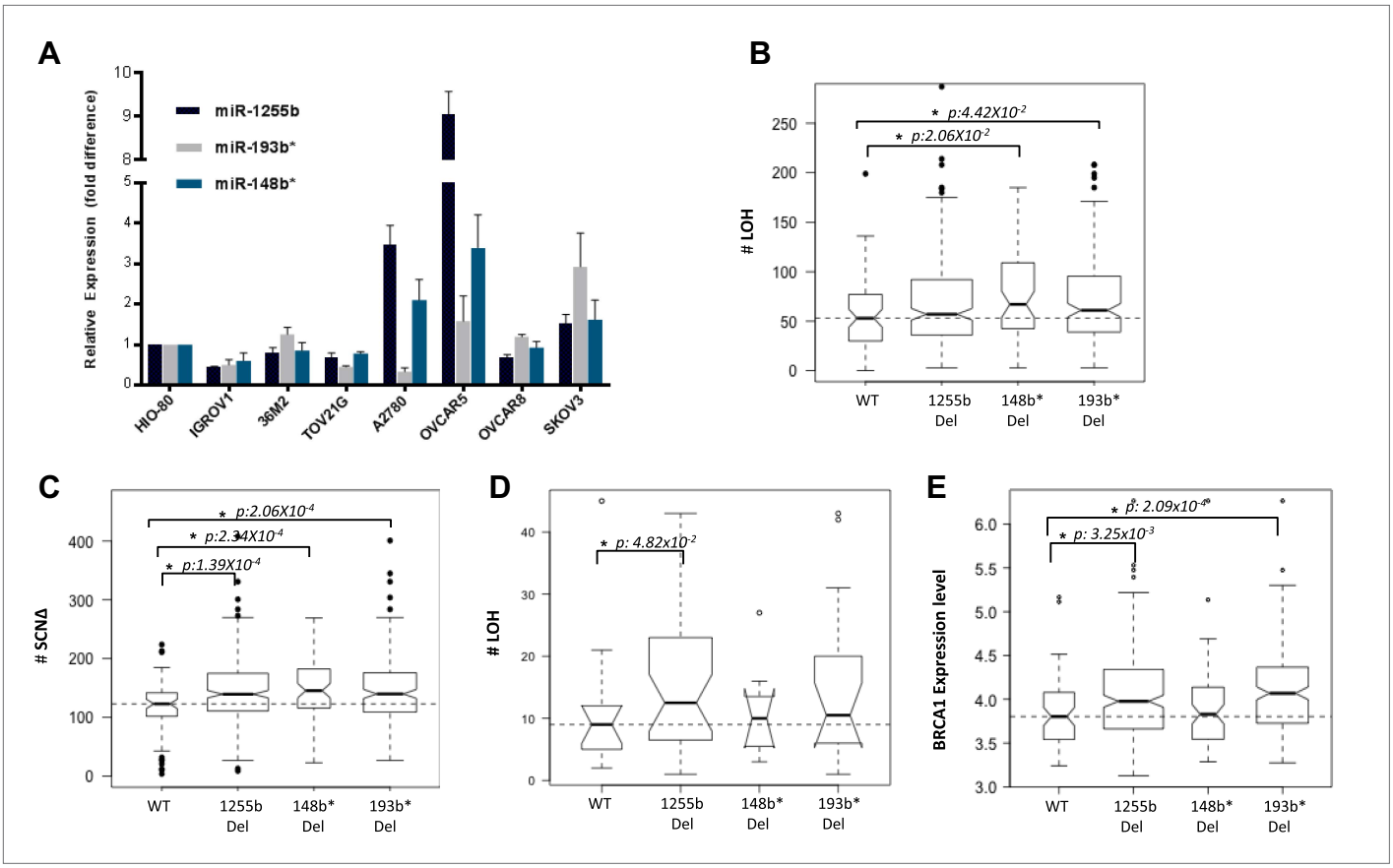

Figure 7. Correlation of LOH with loss of miRNAs. (**A**) miRNA expression profile in a panel of ovarian cancer lines. Endogenous expression of indicated miRNAs was quantified by qRT-PCR (normalized to 5srRNA) and represented relative to non-tumorigenic ovarian epithelial cell, HIO-80. Expression of miR-1255b, miR-193b*, and miR-148b* were detected in these lines. (**B** and **C**) Correlation of LOH with deletion of miRNAs in TCGA data set. Box plots show the frequency of (**B**) LOH or (**C**) somatic copy number amplification or deletion (SCNΔ) in the 418 high-grade serous ovarian tumors from TCGA that have no amplifications or deletions of any of these 3 miRNAs (WT), against those with deletion of 1255b (either −1 or −2), 148b* or 193b*. The LOH events are >1 Mb. (**D**) Correlation of LOH with deletion of miRNAs in DF/HCC data set. Box plot shows the frequency of LOH in 47 high-grade serous ovarian tumors that have no amplifications or deletions of any of these 3 miRNAs (WT), against those with deletion of miR-1255b (either 1 or 2), miR-148b* or miR-193b*. The LOH events are >1 Mb. (**E**) Correlation of BRCA1 expression with deletion of miRNAs in TCGA data set. Box plot shows expression levels of BRCA1 in the 418 high-grade serous ovarian tumors from TCGA that have no amplifications or deletions of any of these 3 miRNAs (WT), against those with deletion of miR-1255b (either 1 or 2), miR-148b* or miR-193b*. In (**B**–**E**), statistical significance was calculated using one tailed Mann Whitney's U test and significant differences ($p<0.05$) indicated with asterisk. Width of the bars indicates the number of samples. The horizontal line indicates the median of the WT set.

DOI: 10.7554/eLife.02445.015

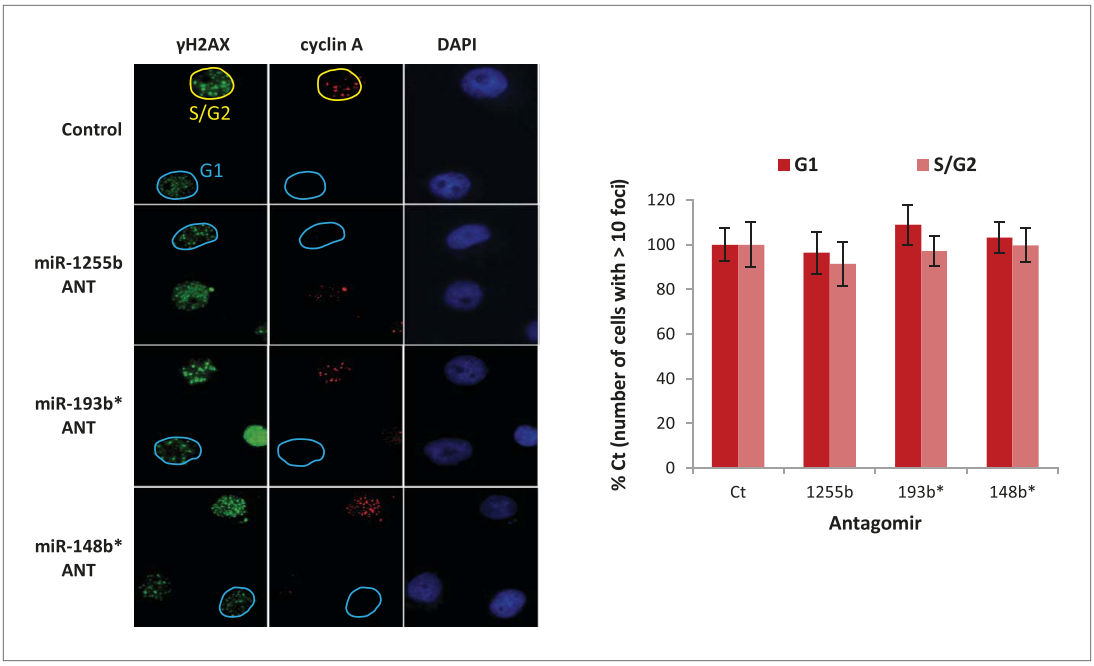

Figure 7—figure supplement 1. miRNA dependent regulation of DSB repair during cell cycle.

DOI: 10.7554/eLife.02445.016

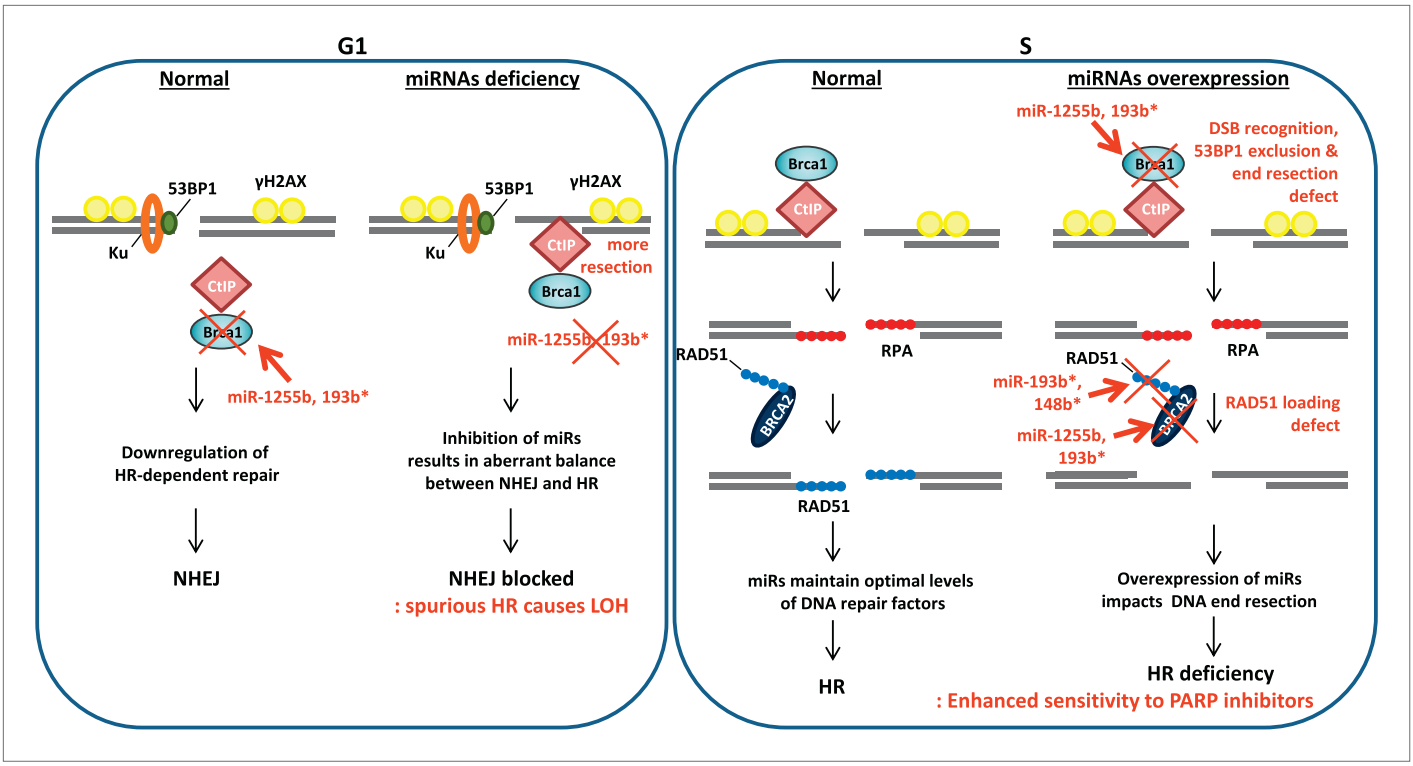

Figure 8. A model of miRNA dependent regulation of DSB repair during cell cycle. Model of miRNA-dependent regulation of DSB repair during cell cycle. The balance of HR and NHEJ in dividing cells is crucial for efficient DSB repair. NHEJ is the preferred pathway in the G1 phase with 53BP1 and the Ku complex binding the broken DNA end. miRNAs (such as miR-1255b and miR-193b*) suppress HR factors, particularly BRCA1, preventing end resection of the DNA lesions. However, when these miRNAs are inhibited or deleted it may disrupt the correct choice of DSB repair pathway. Ectopic over expression of BRCA1 will allow CtIP-mediated resection in G1 cells, preventing NHEJ. Furthermore, HR-mediated repair in G1 is detrimental to cell health as it would lead to LOH. In S-phase, DSBs are predominantly repaired by HR and down-regulation of miRNAs targeting BRCA1, BRCA2 and RAD51 may be important in ensuring efficient HR-mediated DSB repair. Over-expression of miRNAs (such as miR-1255b, miR-193b*, and miR-148b*) targeting BRCA1, BRCA2 and RAD51 in the S phase will impede various steps of HR, and the HR deficiency will sensitize these cells to PARP inhibitors.

DOI: 10.7554/eLife.02445.017